BRAIN
ORIGINAL ARTICLE

In vitro ictogenesis is stochastic at the single neuron level

Lauren A. Lau,[1,2] Kevin J. Staley[1,2,†] and Kyle P. Lillis[1,2,†]

[†]These authors contributed equally to this work.

Seizure initiation is the least understood and most disabling element of epilepsy. Studies of ictogenesis require high speed recordings at cellular resolution in the area of seizure onset. However, *in vivo* seizure onset areas cannot be determined at the level of resolution necessary to enable such studies.

To circumvent these challenges, we used novel GCaMP7-based calcium imaging in the organotypic hippocampal slice culture model of post-traumatic epilepsy in mice. Organotypic hippocampal slice cultures generate spontaneous, recurrent seizures in a preparation in which it is feasible to image the activity of the entire network (with no unseen inputs existing). Chronic calcium imaging of the entire hippocampal network, with paired electrophysiology, revealed three patterns of seizure onset: (i) low amplitude fast activity; (ii) sentinel spike; and (iii) spike burst and low amplitude fast activity onset. These patterns recapitulate common features of human seizure onset, including low voltage fast activity and spike discharges. Weeks-long imaging of seizure activity showed a characteristic evolution in onset type and a refinement of the seizure onset zone. Longitudinal tracking of individual neurons revealed that seizure onset is stochastic at the single neuron level, suggesting that seizure initiation activates neurons in non-stereotyped sequences seizure to seizure.

This study demonstrates for the first time that transitions to seizure are not initiated by a small number of neuronal 'bad actors' (such as overly connected hub cells), but rather by network changes which enable the onset of pathology among large populations of neurons.

1 Department of Neurology, Massachusetts General Hospital, Boston, MA 02114, USA
2 Harvard Medical School, Boston, MA 02115, USA

Correspondence to: Kevin Staley
Department of Neurology, Massachusetts General Hospital, 114 16th Street
Charlestown Navy Yard, MA 02129, USA
E-mail: Staley.Kevin@mgh.harvard.edu

Keywords: epilepsy; seizure onset; ictogenesis; neural networks; calcium imaging

Abbreviations: LAF = low amplitude fast activity; SB = spike burst; SS = sentinel spike

Introduction

Epilepsy, which affects ~1% of the population,[1] is defined as a propensity for spontaneous seizures. Seizures in turn are defined as the 'transient occurrence of signs and/or symptoms due to abnormal excessive or synchronous neuronal activity in the brain'.[2] The unpredictable nature of these events is both the basis of the term 'seizure' as well as one of the most disabling features of the disorder.[3] Understanding seizure initiation, or ictogenesis, is critical for developing prediction schemes[4] as well as mechanistically based

Received March 17, 2021. Revised July 13, 2021. Accepted July 30, 2021. Advance access publication August 25, 2021

treatments for the large fraction of patients who remain medically refractory.[5] Investigating ictogenesis at cellular resolution is the focus of this study.

Unfortunately, ictogenesis is difficult to study. First, seizures occur spontaneously and often unpredictably so that infeasibly long recordings are required to capture them. Many studies have relied on pharmacological manipulations to trigger seizures to gain temporal control; however, the mechanistic relevance of these provoked-seizure models to the mechanisms of spontaneous seizures remains questionable. Second, parsing seizure onset from propagation *in vivo* is impossible with finite recording arrays. Finally, *in vivo* recording methods provide poor spatial sampling, either capturing only population activity (large volume, but low resolution) or the activity of a small number of cells (high resolution, but small volume). To overcome these challenges, we coupled continuous field-potential recordings with chronic, cellular-resolution calcium imaging of an entire neuronal network: hippocampal organotypic slice cultures.[6] This represents a first-of-its-kind study of the activity of a whole epileptic network at cellular resolution. This preparation retains the cytological, anatomical and developmental features of the *in vivo* hippocampus.[7] After 1 week *in vitro*, hippocampal slice cultures generate well-characterized spontaneous seizure-like events[8] that correspond closely to experimental and human epilepsy, including electrographic semiology[8–10] and response to anticonvulsants.[11] Critically, there are no non-recorded inputs to this preparation, as exist *in vivo*. Thus, it is feasible to image the entirety of network activity, ensuring that the earliest pathological activity is captured. In undisturbed slice cultures recorded in the incubator, the calcium activity of hundreds of individual neurons, for dozens of seizures, was followed over several weeks. We used this preparation to address fundamental but previously unanswerable questions regarding ictogenesis, including whether a distinct subpopulation of neurons consistently initiates seizure activity.

Interneurons may comprise one such subpopulation. Interneuron pathologies in epilepsy include interneuron loss,[12,13] failure of inhibitory constraint,[14,15] post-inhibitory rebound spiking[16] and positive shifts in the $GABA_A$ reversal potential.[17–20] Consistent with this last finding, early activation in putative interneurons from unit recordings has been observed in animal models of spontaneous seizures[21,22] and patients with temporal epilepsy,[23] and from optogenetically identified interneurons in chemoconvulsant-induced seizures[24] (although acute chemoconvulsant-induced activity may differ from spontaneous epileptic activity[25]). Here we find that interneurons activate earlier during ictogenesis compared to principal cells, consistent with a possible pro-ictal effect of interneurons during seizure onset.

Finally, we used our unique ability to track the activity of individual neurons across multiple seizures to test whether a subpopulation of neurons consistently activates earliest. Superconnected hub cells are one such possibility. These GABAergic interneurons have been observed in the developing hippocampus and show high levels of functional connectivity, with extensive, long-range arborizations, which are maintained into adulthood.[26,27] Modelling studies have suggested a role for hub cells in generating ictal events.[28–30] If hub cells were responsible for driving the transition to seizure onset, they should consistently be among the earliest ictal activators. Indeed, multiunit recordings have suggested repeatable patterns of seizure propagation *in vivo*.[31,32] Alternatively, it has been proposed that ictogenesis may result from re-entrant activity in networks with small-world connectivity, where all neurons primarily have local connections, with a smaller number of long-range projections.[6,33] This model would predict non-stereotyped seizure onsets. Here, we found that consecutive seizures begin with highly variable neuronal activation sequences indicating that ictogenesis is not necessarily driven by hub cells. Re-entrant activity cannot be studied directly with the current calcium imaging approach, but our findings are consistent with a prediction of transitions to seizure being characterized by stochastic onset sequences at cellular resolution. This finding centres the requirement to view and treat seizure onset as a network phenomenon.

Materials and methods

Study design

This study was designed to capture spontaneous seizure activity, across an entire epileptic network at neuronal resolution. A recording paradigm was designed to balance the need to capture high-resolution, spontaneous activity, with the limitations in acquiring, storing and processing very large datasets, see the Supplementary material for full details.

Here, 85-s long, high-resolution 'movies' of calcium activity were obtained, once every 6 h. Activity was sampled from the same slices for over 3 weeks. Slice health was confirmed by robust calcium activity, and stability of fluorescently labelled neurons. In total, 10 slice cultures were included in the analysis, which came from four animals (one to four slices were used per animal). Data were obtained from three independent imaging cohorts. For the single cell analysis, there was no significant difference in the intra- versus inter-animal variability, confirming the validity of treating each slice culture as an independent data-point (Supplementary Fig. 8C).

Animals

All animal protocols were approved by the Massachusetts General Hospital Institutional Animal Care and Use Committee. DLX-cre mice (Jackson Laboratory, stock number 008199) of either sex were used for this study. Mouse pups remained in the home cage with the dam under standard husbandry conditions until postnatal Day (P) 6–8 when organotypic slice cultures were prepared (see below).

Virus delivery by intracerebroventicular injection

Intracerebroventicular (ICV) injections were performed as described by Glascock *et al.*[34] Viral solutions of 10 µl each of AAV9-hSyn-GCaMP7f and AAV9-FLEX-CAG-tdTomato (Addgene; #104488 and #28306, respectively) were prepared with 0.05% trypan blue for visualization of the injection site. Newborn DLX-cre mouse pups (P1–2) were anaesthetized via hypothermia and viruses were delivered into the ventricles (one virus per hemisphere) using a glass pipette, see full details in the Supplementary material.

Preparation of organotypic slice cultures

Organotypic slice cultures were prepared from P6-P8 DLX-cre mice of either sex using the membrane insert technique[35] for imaging, see the Supplementary material for full details.

Chronic calcium imaging

On the day of slice culture preparation, slices were transferred to the custom imaging system, an inverted microscope constructed inside of a CO_2 incubator,[6] see the Supplementary material for full details. Slices were imaged every 6 h, and each recording included a z-stack of red fluorescence (15 10-µm steps) to record the anatomical distribution of interneurons and an 85-s time series of green fluorescence at 35 Hz from a single, central, z-plane to record the spatiotemporal dynamics of calcium activity.

Electrophysiology

In some experiments, imaging was paired with electrical recordings of the extracellular field potential, see the Supplementary material for full details.

Calcium imaging data analysis

Preprocessing of calcium imaging

Active, GCaMP+ cells were identified from the frame-to-frame standard deviation projection (STD) of the high-resolution calcium recordings. The STD projection highlights pixels with dynamic signal. The Fiji plugin TrackMate[36] was used to automatically select 40 μm^2 regions of interest corresponding to the soma of active cells from the STD projection (Supplementary Fig. 4A), and calcium signal was extracted as the mean pixel intensity of each region of interest. GCaMP7f is expressed in both the soma and neuropil of neurons, which can create challenges when trying to separate the calcium signal from an individual neuron versus the surrounding neuropil. Calcium traces were corrected for neuropil contamination by subtracting the mean intensity of an annulus region of interest of the local neuropil fluorescence surrounding the neuronal region of interest. Empirically, we found that the optimal removal of contaminating signal, without overcorrection was achieved by: $F_{raw} - 0.9 \times F_{neuropil}$ to provide the neuropil corrected *F*-value ($F_{np\text{-}corrected}$). Without neuropil subtraction, the diffuse and large neuropil fluorescence can give a false impression of extreme synchrony across all neurons (Supplementary Fig. 4B–E). Calcium traces were normalized on a frame-by-frame basis as $\Delta F/F$, see the Supplementary material.

Activation threshold

The threshold for being considered in the active state was determined on a cell-by-cell basis, as mean + 3 standard deviations (SD) from a baseline period of 100 frames (~3 s) without ictal or epileptiform activity. Threshold values were used to determine the onset time (first threshold crossing) and percentage of time spent in the active state (total time above threshold in a predefined window). We compared threshold to onset time, to ensure that the timing of ictal onset was not correlated with a cell's threshold value (Supplementary Fig. 3E and F).

Random, shuffled and early activator surrogate analyses

To test the hypothesis that seizure onset is stochastic, three control analyses were performed to compare to the experimentally obtained mean minimum onset. The first was to compare the experimentally obtained mean minimum onset, to the mean minimum obtained from a paired number of randomly generated sequences. For example, the mean in Fig. 6A is obtained from the mean normalized onset rank of 1100 neurons across six seizures. A uniformly distributed random sequence of 1100 numbers was generated and then peak normalized. This was done six times and the peak normalized sequences were averaged (so each of the 1100 positions had six values that were averaged). The minimum from this set of means is therefore the minimum value you would expect from a set of sequences with a random distribution of values sequence to sequence. This analysis was repeated for 50 iterations and the minimums were averaged to produce the final mean minimum onset of random sequences. Each slice has one such 'mean minimum onset of random sequences' per seizure onset type.

The experimental data were also compared to activity shuffled data. Here the experimental data were shuffled in a sliding window of 500 ms. The activity thresholded data were used for the shuffling, such that each cell had a binary above or below threshold value at each time point. Within each 500 ms window, the exact time above threshold would be randomized, but the total amount of time above threshold would be kept the same. Each cell was shuffled independently. The shuffled data were then used to calculate onset ranks for each cell, and the mean minimum onset was calculated as before (with 50 iterations to calculate the mean minimum onset of activity shuffled data; one per slice per onset type).

Finally, the experimental data were compared to a sequence of onsets where a set of early activators was artificially added into the sequence. Here for a set of seizures (where a set of seizures = all the seizures of the same onset type in a slice), 50 cells are chosen at random to be 'early activators'. In each seizure within the set, the same 50 cells were given a new onset time that was within the first 200 ms (exact onset time was randomized) and new sequences of onset ranks was generated. These sequences were then averaged to calculate the mean minimum onset across all the seizures. This was done for a new set of 50 cells in each of the 50 iterations, which was used to calculate the mean minimum onset that would be predicted with a subset of consistently early activating cells.

Immunohistochemistry

Hippocampal organotypic slice cultures were prepared and stained as described by Gogolla *et al.*,[37] see the Supplementary material for full details. Cell counting was performed in ImageJ and Cell Profiler.[38]

Data presentation and statistics

All data means from $n > 10$ are presented as box and whisker plots. When $n < 10$, data are presented as a bar chart of mean ± SEM with dots for individual points. Bee-swarm plots were also used to allow for visualization of overlapping data points (adapted from Stevenson[39]). Two-tailed *t*-tests were used to compare means, with Holm–Bonferroni correction applied for multiple comparisons where appropriate. The variability in onset sequences from seizure to seizure was assessed by the Kendall rank coefficient, see the Supplementary material. All analyses were performed in ImageJ (Fiji) and MATLAB.

Data availability

Data generated from this study is available on reasonable request from the corresponding author.

Results

Ictogenesis at cellular resolution

To investigate the activity of individual neurons during ictogenesis, we used our newly developed continuous single-photon imaging system to chronically record GCaMP7-based neuronal calcium activity. Slice cultures were maintained undisturbed in the imaging system for the duration of these month-long experiments. GCaMP7f was expressed across all neuronal subtypes and locations (Supplementary Fig. 2A and B), by *in vivo* ICV injection of AAV9-hSyn-GCaMP7f, paired with interneuron labelling by ICV injection of AAV9-FLEX-CAG-Tdt in DLX-cre mice at P1–2. Using this approach, we were able to resolve ~800–1200 GCaMP+ neurons per slice culture (Supplementary Fig. 2A). Organotypic hippocampal slice cultures contain ~10 000 NeuN+ neurons per slice culture (9863 ± 910 NeuN+ neurons per slice; $n = 3$ organotypic slice cultures at DIV7; Supplementary Fig. 2H), of which 6119 ± 856 are Phospho S6+. If we consider the NeuN/Phospho S6+ neurons as

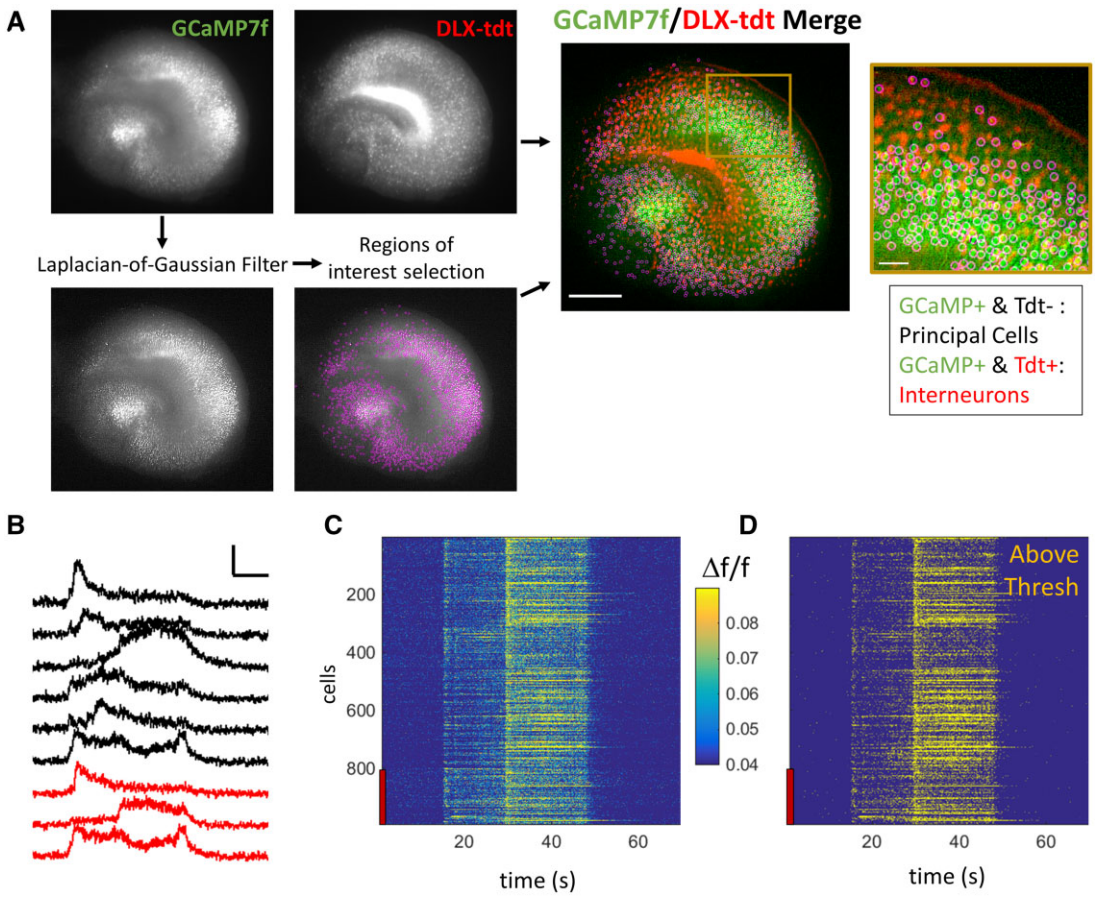

Figure 1 Ictogenesis at cellular resolution. (**A**) Representative images of Syn-driven expression of GCaMP7 (STD projection of GCaMP7 activity) and DLX-cre driven tdTomato labelling of interneurons. Scale bar on merge image = 500 μm. Scale bar on zoom in = 50 μm. Laplacian-of-Gaussian Filter is applied to GCaMP images before automatic region of interest selection (pink circles). All tdTomato+/GCaMP+ cells were considered interneurons (IN) and tdTomato–/GCaMP+ cells as principal cells (PC). (**B**) Example traces from nine individual neurons (black = principal cells, red = interneurons) during a seizure event. Scale bar = 0.1 Δ*f*/*f* and 10 s. (**C**) Raster plot of Δ*f*/*f* for all detected neurons from same seizure as **B**. Red bar indicates interneurons. (**D**) Raster plot of same neurons as **C**, where yellow = frames above active threshold. Tdt/tdt = tdTomato.

the total healthy, transcriptionally active population, this strategy results in GCaMP expression in ∼23% of active neurons. This relatively sparse expression was purposeful to allow for single cell detection with single-photon imaging. Conversely, FLEX-cre driven tdTomato expression under a CAG promoter was used to robustly label interneurons. In total 2000–4000 tdTomato+ interneurons were identified per slice, 26.4% (± 2.1, $n = 10$) of which were also GCaMP+ (the remaining tdTomato+ interneurons were not assigned a region of interest). 35.7% (± 4.1%, $n = 10$) of GCaMP+ neurons were identified as interneurons by co-localization of tdTomato (Fig. 1A), where all GCaMP+/tdTomato+ cells were considered to be interneurons and GCaMP+/tdTomato– cells were considered to be principal cells. *Post hoc* staining of GAD67 in DLX-cre slices with FLEX-tdTomato expression revealed that 93.5% ± 0.5 of tdTomato+ cells were also positive for GAD67 ($n = 8$ organotypic slices; Supplementary Fig. 2E and F). Most tdTomato+/GAD67– cells were in the hilus, which is known to contain a small population of GAD65+/GAD67– interneurons,[40,41] suggesting that DLX-tdTomato expression was highly specific for interneurons. We also found that 83.8% ± 1.7 of GAD67+ cells were also tdTomato+ ($n = 8$ organotypic slices, Supplementary Fig. 2E). Therefore, a small percentage of interneurons may have been falsely identified as principal cells due to lack of tdTomato expression.

We recorded 85-s long series of high-resolution images at 35 Hz to capture the spatiotemporal dynamics of calcium activity. These 'movies' were obtained from each slice culture once every 6 h, beginning on the day of culture preparation [day *in vitro* (DIV) 0] and continuing for >3 weeks (Supplementary Fig. 1A). Cellular-resolution calcium activity (Supplementary Fig. 4) was extracted from individual neurons (Fig. 1A–C), with the goal of parsing the cellular activity leading up to seizure initiation. Seizure-like events (henceforth referred to as 'seizures') were easily identifiable from the mean Δ*f*/*f* of neuronal calcium activity, as large amplitude (>2× baseline) calcium transients lasting for >5 s. Seizure onset was defined as the period beginning from the earliest detectable rise in mean Δ*f*/*f*, until the local maxima of the Δ*f*/*f* slope that marks the transition to frank seizure. An activation threshold was determined on a cell-by-cell basis (as mean + 3 SD of baseline activity; see Methods) to translate the Δ*f*/*f* calcium signal to a binary above/below threshold signal (Fig. 1D).

Ictal onset patterns

Seizure onset type is often defined by the EEG signature in patient populations. A diverse catalogue of ictal onsets has been characterized from patient EEG[42–46] and computational approaches.[47–49] Here we defined three onset types based on calcium imaging: low amplitude fast activity onset (LAF); sentinel spike (SS); and spike burst and low amplitude fast activity (SB+LAF). LAF onset seizures were characterized by several seconds of low amplitude calcium activity, which preceded high-amplitude, hypersynchronous ictal

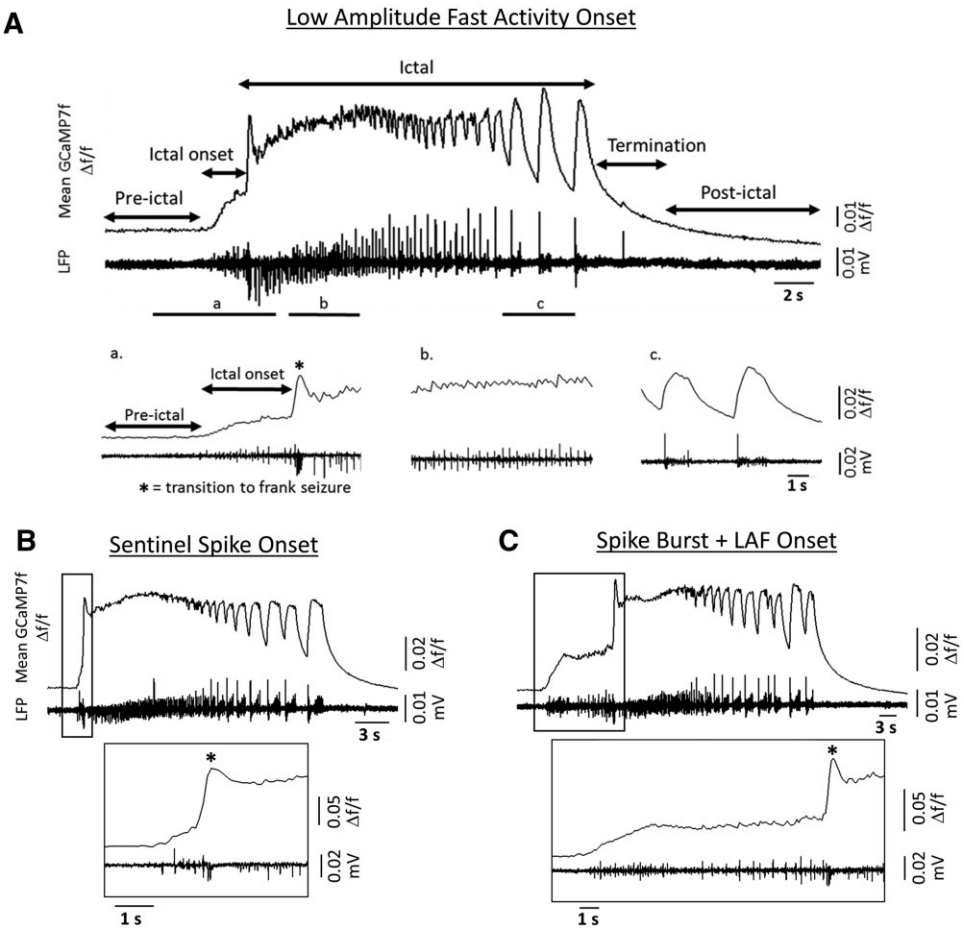

Figure 2 Ictal onset type. (**A**) Representative trace of paired mean Δ*f*/*f* GCaMP7f calcium activity and local field potential activity (LFP) during a low amplitude fast activity onset seizure, with phases of activity labelled. *Bottom* panels show expanded resolution of regions a–c. (**B**) Representative traces of paired mean Δ*f*/*f* and LFP activity for an SS onset seizure. *Bottom* panel shows expanded resolution around ictal onset. (**C**) Same as in **B**, but for an SB + LAF onset seizure.

calcium activity (i.e. the transition to frank seizure). In paired electrical field-potential recordings, LAF onset seizures displayed characteristic low voltage fast activity[23,42,50] (Fig. 2A). SS onset was defined by a brief period of spikes (<1.5 s) before the transition to ictal activity (Fig. 2B). SS onset is reminiscent of the brief pre-ictal discharges, which can be observed from intracranial recordings in some patients with mesial temporal lobe epilepsy.[51] All slice cultures recorded for >3 weeks had both LAF and SS onset type seizures. Finally, ∼60% of slice cultures also displayed SB + LAF onset seizures, which were characterized by one or more high-amplitude spikes, followed by several seconds of low amplitude activity during the onset period (Fig. 2C). Often SB + LAF onset seizures presented with a bi-phasic onset (a single high-amplitude burst of calcium activity followed by several seconds of low amplitude activity). In paired field-potential recordings, this single, high-amplitude calcium spike was revealed to be composed of a brief burst of electrical spiking activity. A similar pattern of SB (followed by low voltage fast activity) onset was occasionally observed from intracranial EEG recordings in patients with temporal lobe epilepsy.[50,52]

Ictal onset: evolution during epileptogenesis

All slice cultures displayed similar evolutions in ictal onset type, where LAF onset was consistently the earliest observed seizure type, followed by SS and SB + LAF (Fig. 3A and Supplementary Fig. 5A). Individual slice cultures alternated among the onset types, i.e. onset types could alternate from one seizure to the next, so that seizure onset did not evolve from one type to the next in an absolute manner. We observed a general trend towards increased peak Δ*f*/*f* and seizure duration over time, but did not find an independent relationship between onset type and ictal amplitude or duration (Supplementary Fig. 5B and C). The inter-ictal interval decreased with days *in vitro* (Fig. 3C), consistent with the idea that the severity of epilepsy increased over time in organotypic slice cultures. The mean inter-ictal interval during days when only LAF onset seizures were observed was 301.8 s ± 34.1 s (Fig. 3D; $n = 32$ days from 10 slices, from four animals). This was significantly longer than days with mixed seizure onset (198.6 s ± 14.9 s, $n = 40$ days; $P < 0.05$ *t*-test with Holm–Bonferroni correction for multiple comparisons) or with SS/SB + LAF onset only (148.2 s ± 15.1 s, $n = 14$ days; $P < 0.05$ *t*-test with Holm–Bonferroni correction for multiple comparisons). These results indicate a correlation between the more mature forms of ictal onset (SS and SB + LAF) and more frequent seizures.

Seizure onset zone

Early during epileptogenesis, seizure onset did not initiate in a regionally defined manner. However, all slice cultures developed regionally specific seizure onset zones by the second week *in vitro* (Fig. 4A and B). We consistently observed that later seizures began

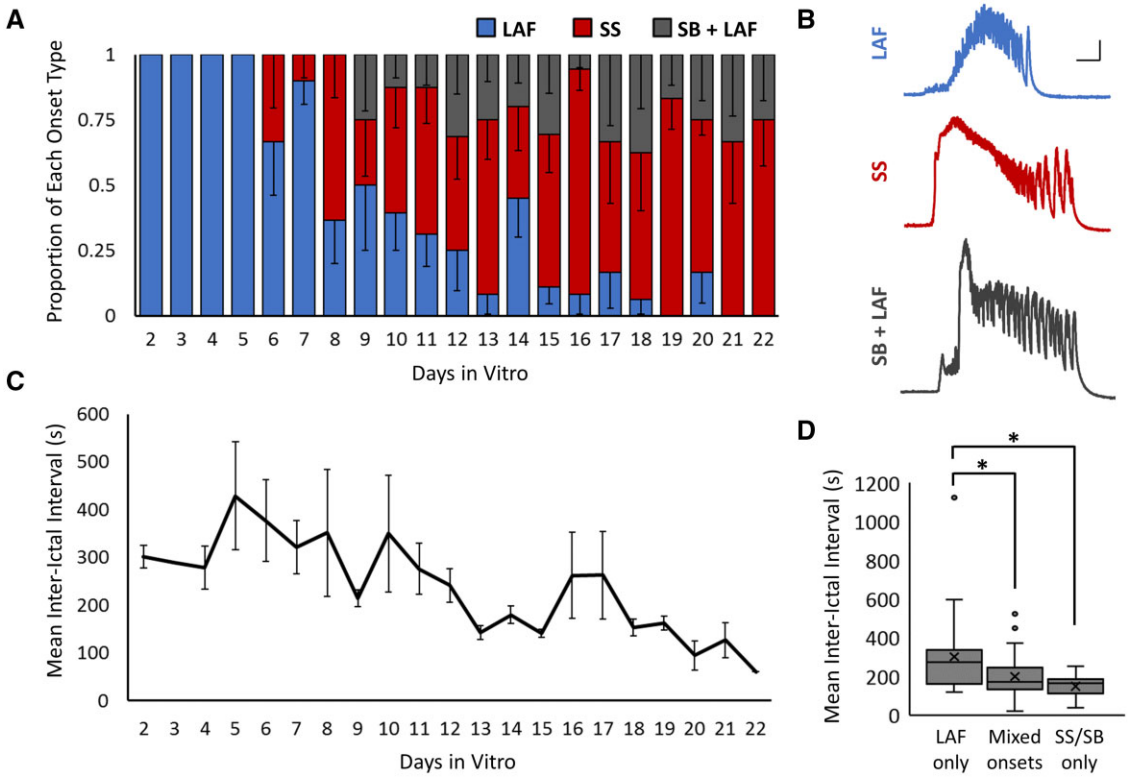

Figure 3 Evolution of ictal onset type. (**A**) Proportion of each seizure onset type by days *in vitro* [$n = 150$ seizures, from 12 slice cultures (from four animals)]. Blue = low amplitude fast activity onset (LAF), red = sentinel spike onset (SS) and grey = spike burst + low amplitude fast onset (SB + LAF). (**B**) Representative $\Delta F/F$ calcium traces of each ictal onset type, all from the same slice culture. Scale bar = 5 s and 0.1 $\Delta F/F$. (**C**) Mean inter-ictal interval by days *in vitro*, $n = 12$ slice cultures. (**D**) Mean inter-ictal interval during days when only LAF onset seizures were present, days with mixed seizure onsets, or days with only SS and/or SB + LAF onset. Box = inner-quartile range (IQR); line = median; X = mean; dots = outliers, >1.5 of the IQR. $n = 32$, 40 and 14 days, from nine slices and four animals; *$P < 0.05$ Student's *t*-test, with Holm–Bonferroni correction for multiple comparisons.

with the earliest activity in the CA1, and often included early activity in dentate gyrus and hilus as well (Fig 4C; 21.7% ± 9.2 CA1, 8.8% ± 6.0 CA1 and dentate gyrus, 69.4% ± 12.7 CA1, dentate gyrus and hilus, $n = 99$ seizures from nine slice cultures). Although most slice cultures displayed a single seizure onset zone (Fig. 4D; 62.5% of slices had a single seizure onset zone), 25.0% of slice cultures had two and 12.5% had three seizure onset zones.

Does a specific subpopulation of neurons drive seizure onset?

We first considered if there was a cell type difference in onset time for interneurons versus principal cells during ictal onset. In time windows distant from ictal events (>30 s before the next seizure), both principal cells and interneurons showed low levels of activity, with no significant difference between the two populations [Supplementary Fig. 6A; 0.26% and 0.26% ± 0.003, time above threshold in a 5-s window, 95% CI (0.256, 0.268) and (0.254, 0.270), $n = 46$ inter-ictal windows, $t(45) = 0.0313$, $P = 0.48$]. To test the hypothesis that interneurons activate earlier in ictogenesis, an onset time was calculated for all neurons during each seizure, where onset time was the first threshold crossing during onset or frank seizure. On average, interneurons were found to activate earlier than principal cells (Supplementary Figs 6B, C and 7B and C),but to a relatively modest degree [mean onset time: 1.70 and 1.62 s ± 0.01, for principal cells versus interneurons, respectively; 95% CI (1.68, 1.72) and (1.59, 1.64), $n = 138$ seizures, $t(137) = 3.676$, $P < 0.001$, paired *t*-test]. When mean onset time was calculated per region, we found that interneurons preceded principal cells specifically in CA3 [mean onset time: 2.30 and 2.19 s ± 0.02; 95% CI (2.28, 2.33) and (2.17, 2.21), $n = 125$ seizures, $t(124) = 3.392$, $P < 0.001$, paired *t*-test] and CA1 [mean onset time: 1.47 and 1.40 s ± 0.01; 95% CI (1.45, 1.48) and (1.38, 1.41), $n = 125$ seizures, $t(124) = 3.038$, $P < 0.001$, paired *t*-test]. This finding is consistent with the prediction of early interneuron activation during ictogenesis[53]; however, the subtlety of this difference argues for a more careful dissection of possible cellular initiators of seizure onset as follows.

To determine whether a subpopulation of neurons, such as a subclass of interneurons or hub cells, are critical to ictogenesis, we next took advantage of our longitudinal tacking of neurons and considered the onset sequence of neurons across multiple seizures. For each seizure, neurons were ranked from 1 to $N - 1$ according to the order of first activation during ictal onset, where neurons that first activated in the same frame (of ∼28 ms) were assigned the same rank. All neurons that remained inactive during ictal onset were ranked 'N' (i.e. inactive neurons were given the highest rank). As the value of N differed across seizures, onset rank was peak normalized by N to allow for comparisons in activation sequence across seizures. Despite finding repeatable regions of seizure onset (Fig. 4), the activation sequence of individual neurons was found to be highly variable across seizures (Fig. 5A). We quantified the Kendall rank correlation of neuronal onset sequences and found a weak correlation in the sequence of activation seizure to seizure for all types of ictal onset (Fig. 5B and C; mean correlation between seizures per slice culture: 0.20 ± 0.02, 0.14 ± 0.05 and 0.18 ± 0.03; $n = 8$, 5 and 6 slice cultures for LAF, SS and SB + LAF onset). Low sequence correlation was also found when comparing onsets for interneurons or principal cells [Supplementary Fig. 7B; 0.17 ± 0.02 and 0.17 ± 0.07 (principal cells versus interneurons for LAF onset), 0.13 ± 0.04 and 0.19 ± 0.07 (SS

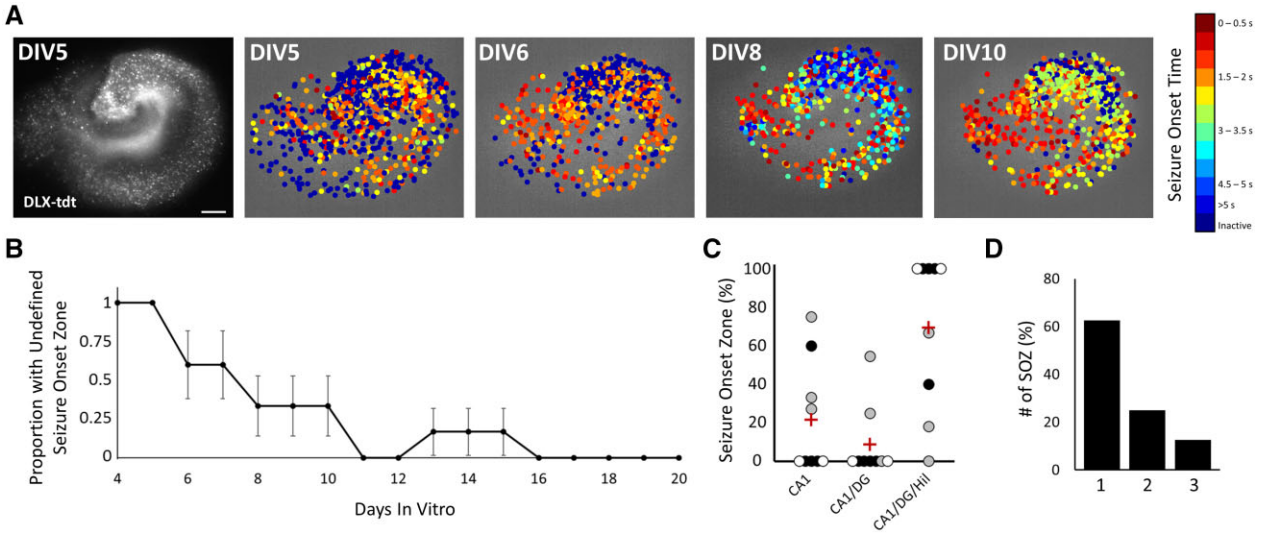

Figure 4 Evolution of seizure onset zone. (**A**) *Left* image shows the overall anatomy of an example slice with DLX-cre driven tdTomato labelling of interneurons. Scale bar = 100 μm. Other panels show the onset time of individual neurons within the example slice over four different seizures spanning DIV5 to DIV10. (**B**) Plot of the proportion of seizures with an undefined seizure onset zone over time. $n = 6$ slice cultures (all slices with early seizures captured by high-resolution imaging). (**C**) Bee-swarm plot of percentage of seizures from each slice with each seizure onset zone: CA1, CA1 and dentate gyrus (DG), or CA1, DG and hilus (Hil). Red cross = mean; $n = 9$ slices; colour of dot indicates slices from the same animal. (**D**) Percentage of slices with one, two or three observed seizure onset zones (SOZ); $n = 9$ slices.

onset), and 0.21 ± 0.02 and 0.18 ± 0.03 (SB + LAF onset)], and when separating neurons based on region (Supplementary Fig. 7C; hilus: 0.03 ± 0.05, dentate gyrus: 0.01 ± 0.06, CA3: 0.13 ± 0.03 and CA1: 0.09 ± 0.04 for LAF onset seizures; hilus: 0.10 ± 0.04, dentate gyrus: 0.06 ± 0.04, CA3: 0.10 ± 0.03 and CA1: 0.06 ± 0.03 for SS onset seizures; hilus: 0.07 ± 0.04, dentate gyrus: 0.14 ± 0.06, CA3: 0.11 ± 0.01 and CA1: 0.10 ± 0.03 for SB + LAF onset seizures). Low sequence correlation was similarly robust to alternate methods of defining the onset of activity, including determining onset based on exceeding a constant threshold of calcium activity for all cells (Supplementary Fig. 7D; Kendall rank correlation: 0.23 ± 0.03, 0.06 ± 0.09 and 0.23 ± 0.03) and onset determined using lowpass filtered calcium traces to determine when the activity threshold was exceeded (Supplementary Fig. 7E; 0.18 ± 0.02, 0.05 ± 0.10 and 0.19 ± 0.03). To test whether synaptic or dendritic activity might be more stereotyped from seizure to seizure, we also compared the seizure-to-seizure activation rank for non-neuropil subtracted data (Supplementary Fig. 7F; 0.33 ± 0.03, 0.23 ± 0.05 and 0.30 ± 0.04), and within the neuropil alone (Supplementary Fig. 7G, –0.11 ± 0.20, 0.16 ± 0.04 and –0.003 ± 0.08, $n = 3$, 14 and 16 seizures). The non-subtracted and neuropil only data shows a trend towards higher sequence correlation, probably due to our inability to resolve the activity of individual cellular elements in the neuropil, so that activity in the neuropil appeared more synchronous.

As another test for a subpopulation of neurons whose activation consistently initiated seizure onset, we calculated the cumulative distribution function (CDF) of the normalized onset time for single seizures and for the mean normalized onset of neurons across multiple seizures (Fig. 6A). CDFs were also computed from the mean of a paired number of randomly generated series and from sequences with shuffled activity, where activity was shuffled within a sliding window of 500 ms, but mean activity was kept the same (Fig. 6B, see the 'Materials and methods' section). In CDFs generated from single seizures, the minimum onset value will always be zero for the earliest activators. If these same neurons were the earliest activators for multiple seizures, then the minimum onset value of the mean CDF would also be zero or nearly zero. Instead, we found that the minimum normalized onset from the mean onsets across multiple seizures was significantly higher than zero (0.06 ± 0.01, 0.27 ± 0.08 and 0.05 ± 0.01; $n = 8$, 5 and 6 slices for LAF, SS, and SB + LAF onset seizures, respectively) and was not significantly different than the mean minimum values obtained from randomly generated sequences (0.06 ± 0.001, 0.12 ± 0.06 and 0.04 ± 0.001) or from activity shuffled data (0.05 ± 0.001, 0.12 ± 0.02 and 0.03 ± 0.01). A mean minimum onset was also calculated from a random subselection of 100 cells, repeated across 50 iterations (Supplementary Fig 8B; 0.13 ± 0.01, 0.34 ± 0.05 and 0.13 ± 0.01, for LAF, SS and SB + LAF, respectively). This subset analysis revealed an even higher mean minimum onset compared to the full experimental dataset for LAF ($P < 0.001$) and SB + LAF onset seizures ($P < 0.001$, *t*-test). This highlights the need for a large sample size to capture the true early activity.

We also performed a surrogate analysis to approximate a CDF with a population of early activators. To do so, 50 cells were chosen at random to have an onset time within the first 200 ms (exact onset time was randomized) in every seizure in which that cell was detected (Fig. 6B, see the 'Materials and methods' section). The onset data for the remaining cells was unchanged. The mean minimum onset for this 'early activator' data was 0.01 ± 0.004, 0.02 ± 0.003 and 0.01 ± 0.003 (Fig. 6C), and was significantly less than experimental data ($P < 0.01$, $P < 0.05$ and $P < 0.01$; paired *t*-test, with Holm–Bonferroni correction for multiple comparisons). This value did not change significantly when varying the total number of 'early activators' from 1 to 100 (Supplementary Fig 8A). Together, these data indicate that the mean minimum onset (i.e. average earliest activation during seizure onset) is later than would be predicted if there were a subpopulation of neurons that consistently activated at the beginning of seizure onset.

Finally, we examined the period immediately before seizure onset, to determine whether there were any neurons that were consistently active preceding the population-level changes that mark the beginning of ictal onset. While there were many neurons that were consistently silent in the seconds preceding ictal onset (across all cell types and regions, Supplementary Fig. 8D), no neurons were found that were reliably active in this pre-ictal time period (Fig. 6D). Taken together, these results reveal that different

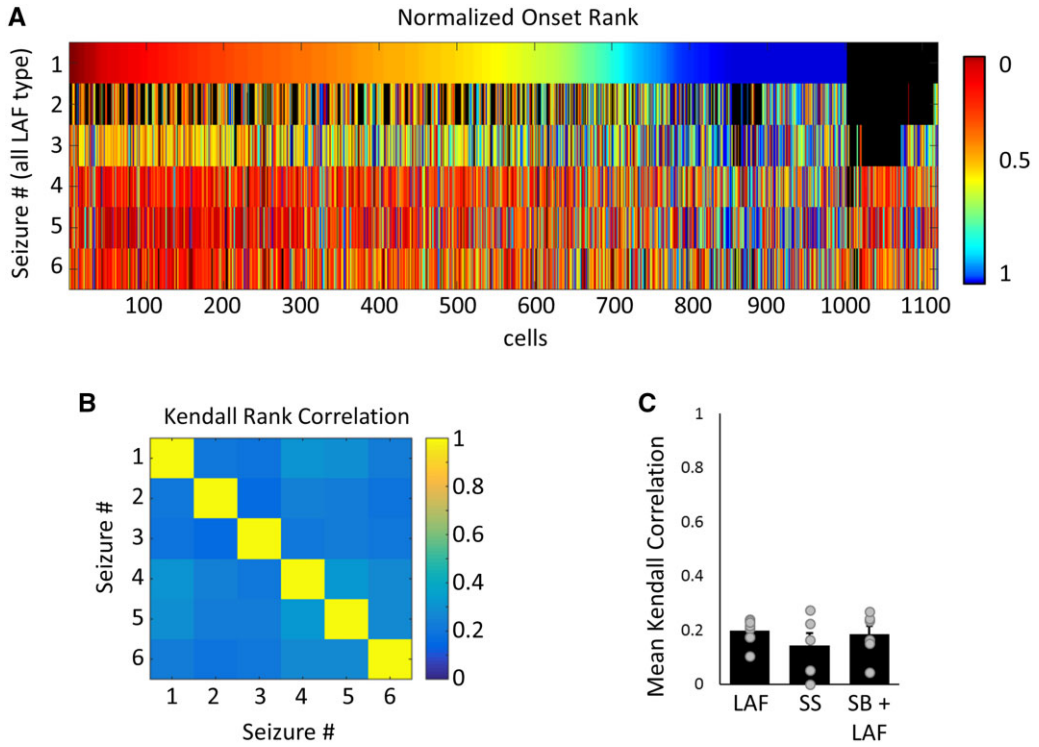

Figure 5 Variable ictal onset sequences seizure to seizure. (**A**) Raster plot of normalized seizure onset rank of individual neurons for six LAF onset seizures. Cells were ordered by onset rank in seizure #1, and subsequent rows indicate the onset time of the same neurons (in the same order) for the following five LAF seizures captured. Colour bar = normalized onset rank; black = neurons not tracked in a given seizure. (**B**) Kendall rank coefficient for seizures in **A**. (Kendall rank coefficient can span –1 to 1, where 1 = perfect positive correlation and 0 = no correlation). (**C**) Mean Kendall rank coefficient by seizure onset type. $n = 8$, 7 and 5 slices for LAF, SS and SB + LAF onset, respectively. Average correlation was calculated for each slice from 2–13 seizures of the same onset type.

sets of neurons are active during early ictogenesis across multiple seizures and argues against the presence of a subpopulation of neurons, either hub cells or interneurons, that consistently drive seizure initiation.

Discussion

In the current study, we used cellular calcium imaging to analyse how spontaneous seizure activity begins in an *in vitro* preparation in which the entire epileptic network was visualized, and to which there were no other inputs. No convulsants were used in these studies. Our chief findings are: (i) we observed three unique patterns of spontaneous ictal onset in our preparation, defined by calcium imaging and electrophysiology: LAF, SS and SB + LAF; (ii) seizure onset evolves in a characteristic manner during epileptogenesis *in vitro*. This includes both a refinement of the seizure onset zone and an evolution in the predominant pattern of seizure onset; and (iii) seizure onset is stochastic at the level of individual neurons.

Seizure onset evolves slowly and predictably

The onset patterns observed here recapitulate features of ictal onsets seen in patient populations. LAF and SB + LAF resemble the commonly observed pattern of low voltage fast activity. Sentinel spike onset closely mimics the brief, pre-ictal discharges that are recorded intracranially from patients with medial temporal lobe epilepsy.[51] Early in epileptogenesis seizures initiated with activity in all subfields of the hippocampus, without a well-defined seizure onset zone. Later in epileptogenesis, preparations demonstrated repeatable anatomical patterns of seizure onset, with the same hippocampal subfields activating in a consistent temporal sequence. Across all hippocampal slices, the earliest activity was observed in CA1 and commonly included early activation of CA1, hilus and dentate gyrus. Nearly all neurons within the slice culture increased activity during ictal onset, suggesting that the entire organotypic slice culture can be viewed as the seizure focus. The activity patterns of ictal onset also evolved in a predictable manner. Early in epileptogenesis, all seizures were of the LAF onset type. Later in epileptogenesis, SS and SB onset were more prevalent. While early seizures were more likely to be both LAF onset type and lack an anatomically defined seizure onset zone, the maturation of onset type and seizure onset zone was on different time scales. Slice cultures continued to generate a high number of LAF onset seizures, even after the development of a clear seizure onset zone. These findings underscore the ongoing nature of epileptogenesis even after the emergence of seizures post-injury.

It is interesting that a small network, such as a single hippocampal slices culture, generates multiple types of seizure onset. It has been proposed that different onset types come from involvement of different brain regions.[54] However, we see here that the same focus can generate multiple onset types, even alternating among different types in a short time span. This suggests that relatively fast acting modulations (on a timescale of minutes to hours) may underlie which onset is generated and that observing multiple ictal onset patterns in a patient may not necessarily indicate multi-focal epilepsy. The overall progression in predominant seizure onset type during epileptogenesis *in vitro* may be most consistent with the findings that clinical seizure onset type varies with degree of hippocampal sclerosis.[55] The evolution of onset type suggests that clinically useful information may be derived from seizure onset type, such as the duration of epilepsy or the maturity of the epileptic focus, and perhaps even the probability of responsiveness to anticonvulsant therapy.[10]

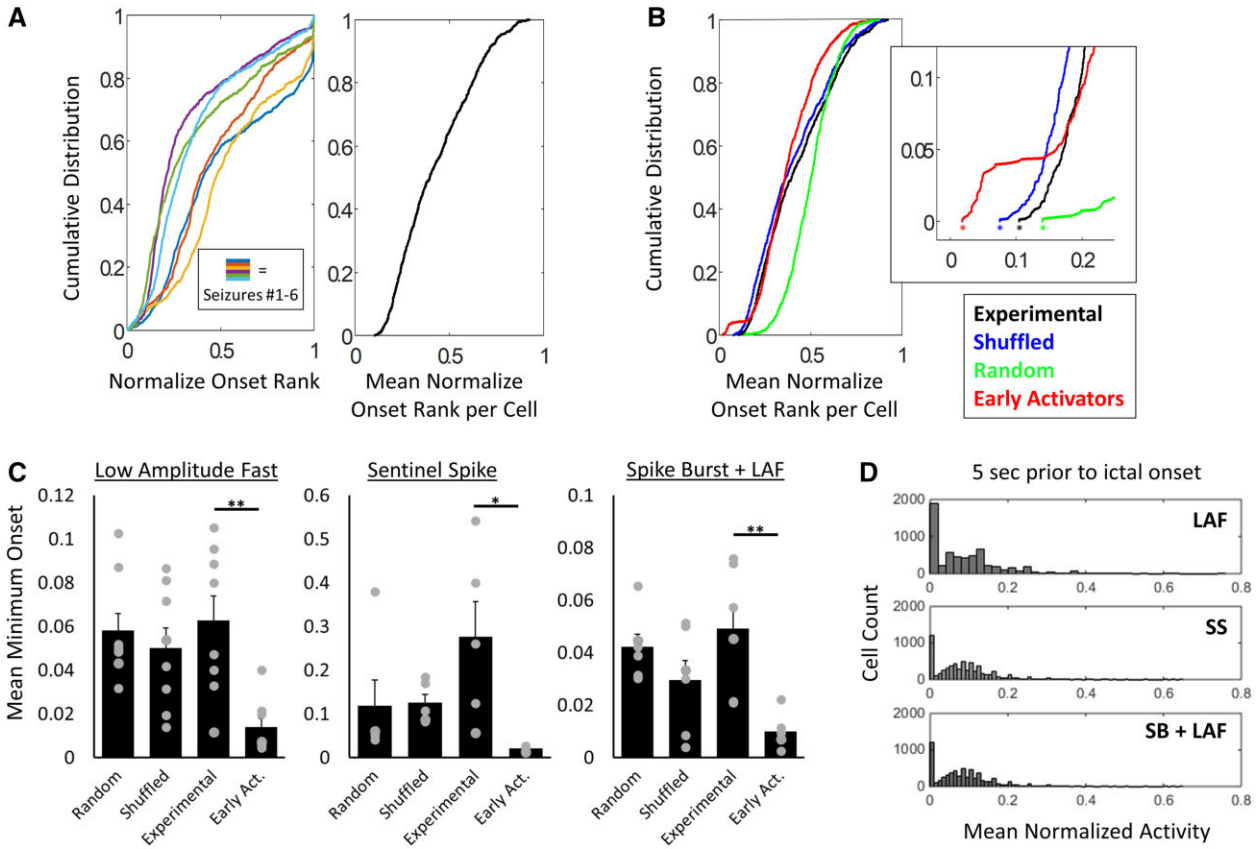

Figure 6 Seizure onset is stochastic at the single cell level. (**A**) Cumulative distribution of normalized onset rank for the six seizures of 5A and the mean onset rank per cell from seizures 1–6 (black). (**B**) Cumulative distribution of mean onset rank per cell from **A** (black), with the activity shuffled (blue), from randomly generated sequences (blue) and from data with early activators added (red). Asterisk indicates the minimum mean onset (i.e. the average rank of the earliest activator across seizures). (**C**) Mean minimum normalized onset rank from eight, seven and five slices for LAF, SS and SB + LAF onset, respectively, (experimental data), and paired shuffled data, random sequences and added early activators. Minimum onset was significantly later for experimental data compared to early activator data; $^{**}P < 0.01$ and $^{*}P < 0.05$, paired *t*-test, with Holm–Bonferroni correction for multiple comparisons. Experimental data compared to random sequences, or activity shuffled data were not significantly different. (**D**) Histograms of mean normalized activity in the 5 s before ictal onset for LAF, SS and SB + LAF onset seizures.

Cellular participation in ictal onset is stochastic

When comparing sequences of activity across multiple seizures, we found that cellular participation in ictal onset is stochastic. If ictogenesis were driven by highly connected hub neurons or other types of 'grandfather cells', we would expect to see the same neurons repeatably leading seizure activity. However, we instead see highly variable neuronal participation at ictal onset. These findings are consistent with our previous modelling suggesting that seizure onsets are stochastic activations of networks that exhibit small-world topology, in which most synaptic connections are local, but some synaptic connections are long-range.[6] Computational studies have proposed a role for hub cells in seizure initiation,[28,29] including recent work identifying 'superhub' cells in imaging-based computational models[30] [which relied on slow (2 Hz) whole brain calcium imaging in zebrafish during seizure induced by GABAA receptor blockade, which substantially alters the propagation of epileptiform activity;[25] or in 4 Hz imaging restricted to the dentate gyrus of chronically epileptic mice]. Superhubs were suggested to play a role in dictating network stability; however, so far there is no computational or experimental evidence that such hubs are directly involved in ictogenesis. In contrast, the current study follows the calcium activity of individual neurons across the entire hippocampus, at high speed (35 Hz), across many spontaneous seizure events to directly demonstrate a pattern of stochastic onset.

If neuronal connectivity patterns are stable relative to the inter-seizure intervals, and there are no external inputs, how can we explain the heterogeneity in cellular seizure onset in this preparation? It is useful to consider factors which can push an epileptic network from normal activity into seizure activity on relatively short timescales. Previous work from our laboratory suggests re-entrant seizure activity can be stochastically engendered in a partially refractory small-world network.[6] Other mechanisms that are consistent with this idea include local increased extracellular potassium or changes in metabolism. Any of these changes may drive an epileptic network into a pro-ictal state, where it becomes possible to trigger a seizure along non-deterministic pathways. The exact conditions at the time when ictal onset is triggered may also underly which onset pattern is manifested.

Conclusions and considerations for the pre-ictal state

We examine here in cellular detail the ictal onset period, a time of unequivocal change that will result in seizure. Our findings are probably not generalizable to all epilepsies. Organotypic hippocampal slice culture is considered a model for post-traumatic epilepsy (PTE), and our findings are probably most applicable to seizures in PTE. Further, we recognize the limitation of the *in vitro*

nature of the investigation. Technologies for large-scale, high-resolution sampling of cellular activity *in vivo* will need to be developed before the current findings can be confirmed *in vivo*. It is possible that the seizure activity within the hippocampal organotypic slice represents a 'microseizure'. Microseizures have been suggested to localize to the seizure initiation site, and to potentially reflect pre-ictal activity.[56,57] Larger scale networks would be needed to confirm if the activity described here reliably propagates or remains focal. However, even if these findings prove to extrapolate primarily to microseizures, they provide a detailed understanding of the earliest transitions to pathological activity within the seizure focus. It remains possible that *in vivo*, hub cells may influence seizure activity; however, we demonstrate that they are not necessary for the generation of spontaneous, recurrent seizures. This study is also not optimized for investigating the contribution of newborn granule cells to seizure onset (as these cells would not express syn-GCaMP). They probably do not drive ictogenesis in our model as the maturation of newborn granule cells[58,59] is slower than the timeline of epileptogenesis; however, this may not hold true *in vivo* where epileptogensis occurs over a longer period of time.

Another limitation is the frequency with which seizures are initiated in hippocampal organotypic slice cultures. This activity is reminiscent of a seizure cluster, and it has been proposed that no true pre-ictal state exists in seizure clusters.[60] Future studies focused on the pre-ictal period could use a model with less frequent seizures. A third limitation is the post-conceptual age of this preparation, which can only reliably be prepared in the first postnatal week. Thus, the stereotyped evolution of seizure onsets in our study could result from epileptogenesis, as well as normal developmental processes. To the extent that normal development versus ongoing epileptogenesis drives the observed changes, we may expect either the age of a patient or the age of the epileptic focus to correlate with the predominate type of seizure onset; these questions can be addressed by clinical studies. The answers could have important clinical implications, including planning surgical resections and predicting successful surgeries as well as later recrudescence.[61]

Our results are consistent with connectivity patterns that can promote seizure activity along multiple pathways at the single neuron level. We suggest that changes during the development of epilepsy in this model may predispose the network towards different modes of ictal onset. Layered on top of these evolutionary changes, we propose that the network enters transient pro-ictal states where it become possible to trigger seizure activity via non-unique patterns of neuronal activity. An important next question is, what are these state changes? Can we identify the critical features of the pre-ictal period to guide seizure prediction and epilepsy surgery? Answering these questions will require a multi-scale approach, where both the network phenomena and underlying cellular mechanisms can be parsed and understood.

Funding

This work was supported by National Institute of Neurological Disorders and Stroke (K.J.S. and K.P.L.). National Institute of Health grants R35 NS116852 and R01NS034700 to K.J.S. National Institute of Health grant R01 NS112538 to K.P.L.

Competing interests

The authors report no competing interests.

Supplementary material

Supplementary material is available at *Brain* online.

References

1. Zack MM, Kobau R. National and state estimates of the numbers of adults and children with active epilepsy - United States, 2015. *MMWR Morb Mortal Wkly Rep*. 2017;66(31):821–825.
2. Fisher RS, van Emde Boas W, Blume W, et al. Epileptic seizures and epilepsy: Definitions proposed by the International League Against Epilepsy (ILAE) and the International Bureau for Epilepsy (IBE). *Epilepsia*. 2005;46(4):470–472.
3. Epilepsy Foundation. Epilepsy Foundation, Landover, MD, 2016.
4. Kuhlmann L, Lehnertz K, Richardson MP, Schelter B, Zaveri HP. Seizure prediction - ready for a new era. *Nat Rev Neurol*. 2018;14(10):618–630.
5. Galanopoulou AS, Buckmaster PS, Staley KJ, et al.; American Epilepsy Society Basic Science Committee and The International League Against Epilepsy Working Group On Recommendations For Preclinical Epilepsy Drug Discovery. Identification of new epilepsy treatments: Issues in preclinical methodology. *Epilepsia*. 2012;53(3):571–582.
6. Jacob T, Lillis KP, Wang Z, et al. A proposed mechanism for spontaneous transitions between interictal and ictal activity. *J Neurosci*. 2019;39(3):557–575.
7. De Simoni A, Griesinger CB, Edwards FA. Development of rat CA1 neurones in acute versus organotypic slices: Role of experience in synaptic morphology and activity. *J Physiol*. 2003;550(Pt 1):135–147.
8. McBain CJ, Boden P, Hill RG. Rat hippocampal slices 'in vitro' display spontaneous epileptiform activity following long-term organotypic culture. *J Neurosci Methods*. 1989;27(1):35–49.
9. Heinemann U, Staley KJ. What is the clinical relevance of in vitro epileptiform activity? *Adv Exp Med Biol*. 2014;813:25–41.
10. Berdichevsky Y, Dzhala V, Mail M, Staley KJ. Interictal spikes, seizures and ictal cell death are not necessary for post-traumatic epileptogenesis in vitro. *Neurobiol Dis*. 2012;45(2):774–785.
11. Berdichevsky Y, Saponjian Y, Park K-I, et al. Staged anticonvulsant screening for chronic epilepsy. *Ann Clin Transl Neurol*. 2016;3(12):908–923.
12. Bouilleret V, Loup F, Kiener T, Marescaux C, Fritschy JM. Early loss of interneurons and delayed subunit-specific changes in GABA(A)-receptor expression in a mouse model of mesial temporal lobe epilepsy. *Hippocampus*. 2000;10(3):305–324.
13. Marx M, Haas CA, Haussler U. Differential vulnerability of interneurons in the epileptic hippocampus. *Front Cell Neurosci*. 2013;7:167.
14. Ziburkus J, Cressman JR, Barreto E, Schiff SJ. Interneuron and pyramidal cell interplay during in vitro seizure-like events. *J Neurophysiol*. 2006;95(6):3948–3954.
15. Schevon CA, Weiss SA, McKhann G, et al. Evidence of an inhibitory restraint of seizure activity in humans. *Nat Commun*. 2012;3:1060.
16. Chang M, Dian JA, Dufour S, et al. Brief activation of GABAergic interneurons initiates the transition to ictal events through post-inhibitory rebound excitation. *Neurobiol Dis*. 2018;109(Pt A):102–116.
17. Cohen I, Navarro V, Clemenceau S, Baulac M, Miles R. On the origin of interictal activity in human temporal lobe epilepsy in vitro. *Science*. 2002;298(5597):1418–1421.
18. Barmashenko G, Hefft S, Aertsen A, Kirschstein T, Köhling R. Positive shifts of the GABAA receptor reversal potential due to altered chloride homeostasis is widespread after status epilepticus. *Epilepsia*. 2011;52(9):1570–1578.

19. MacKenzie G, O'Toole KK, Moss SJ, Maguire J. Compromised GABAergic inhibition contributes to tumor-associated epilepsy. *Epilepsy Res*. 2016;126:185–196.
20. Campbell SL, Robel S, Cuddapah VA, et al. GABAergic disinhibition and impaired KCC2 cotransporter activity underlie tumor-associated epilepsy. *Glia*. 2015;63(1):23–36.
21. Toyoda I, Fujita S, Thamattoor AK, Buckmaster PS. Unit activity of hippocampal interneurons before spontaneous seizures in an animal model of temporal lobe epilepsy. *J Neurosci*. 2015; 35(16):6600–6618.
22. Neumann AR, Raedt R, Steenland HW, et al. Involvement of fast-spiking cells in ictal sequences during spontaneous seizures in rats with chronic temporal lobe epilepsy. *Brain*. 2017; 140(9):2355–2369.
23. Elahian B, Lado NE, Mankin E, et al. Low-voltage fast seizures in humans begin with increased interneuron firing. *Ann Neurol*. 2018;84(4):588–600.
24. Miri ML, Vinck M, Pant R, Cardin JA. Altered hippocampal interneuron activity precedes ictal onset. *eLife*. 2018;7:e40750.
25. Sabolek HR, Swiercz WB, Lillis KP, et al. A candidate mechanism underlying the variance of interictal spike propagation. *J Neurosci*. 2012;32(9):3009–3021.
26. Bonifazi P, Goldin M, Picardo MA, et al. GABAergic hub neurons orchestrate synchrony in developing hippocampal networks. *Science*. 2009;326(5958):1419–1424.
27. Picardo MA, Guigue P, Bonifazi P, et al. Pioneer GABA cells comprise a subpopulation of hub neurons in the developing hippocampus. *Neuron*. 2011;71(4):695–709.
28. Morgan RJ, Soltesz I. Nonrandom connectivity of the epileptic dentate gyrus predicts a major role for neuronal hubs in seizures. *Proc Natl Acad Sci U S A*. 2008;105(16):6179–6184.
29. Petkov G, Goodfellow M, Richardson MP, Terry JR. A critical role for network structure in seizure onset: A computational modeling approach. *Front Neurol*. 2014;5:261.
30. Hadjiabadi D, Lovett-Barron M, Raikov IG, et al. Maximally selective single-cell target for circuit control in epilepsy models. *Neuron* 2021.
31. Wenzel M, Hamm JP, Peterka DS, Yuste R. Reliable and elastic propagation of cortical seizures in vivo. *Cell Rep*. 2017;19(13): 2681–2693.
32. Truccolo W, Donoghue JA, Hochberg LR, et al. Single-neuron dynamics in human focal epilepsy. *Nat Neurosci*. 2011;14(5): 635–641.
33. Netoff TI, Clewley R, Arno S, Keck T, White JA. Epilepsy in small-world networks. *J Neurosci*. 2004;24(37):8075–8083.
34. Glascock JJ, Osman EY, Coady TH, et al. Delivery of therapeutic agents through intracerebroventricular (ICV) and intravenous (IV) injection in mice. *J Vis Exp*. 2011;(56):2968.
35. Stoppini L, Buchs PA, Muller D. A simple method for organotypic cultures of nervous tissue. *J Neurosci Methods*. 1991;37(2): 173–182.
36. Schindelin J, Arganda-Carreras I, Frise E, et al. Fiji: An open-source platform for biological-image analysis. *Nat Methods*. 2012;9(7):676–682.
37. Gogolla N, Galimberti I, DePaola V, Caroni P. Staining protocol for organotypic hippocampal slice cultures. *Nat Protoc*. 2006;1(5): 2452–2456.
38. McQuin C, Goodman A, Chernyshev V, et al. CellProfiler 3.0: Next-generation image processing for biology. *PLoS Biol*. 2018; 16(7):e2005970.
39. Stevenson IH. GitHub repository, 2019. https://github.com/ihstevenson/beeswarm.
40. Houser CR, Esclapez M. Localization of mRNAs encoding two forms of glutamic acid decarboxylase in the rat hippocampal formation. *Hippocampus*. 1994;4(5):530–545.
41. Wang X, Gao F, Zhu J, et al. Immunofluorescently labeling glutamic acid decarboxylase 65 coupled with confocal imaging for identifying GABAergic somata in the rat dentate gyrus-A comparison with labeling glutamic acid decarboxylase 67. *J Chem Neuroanat*. 2014;61–62:51–63.
42. Weiss SA, Alvarado-Rojas C, Bragin A, et al. Ictal onset patterns of local field potentials, high frequency oscillations, and unit activity in human mesial temporal lobe epilepsy. *Epilepsia*. 2016; 57(1):111–121.
43. Foldvary N, Klem G, Hammel J, et al. The localizing value of ictal EEG in focal epilepsy. *Neurology*. 2001;57(11):2022–2028.
44. Perucca P, Dubeau F, Gotman J. Intracranial electroencephalographic seizure-onset patterns: Effect of underlying pathology. *Brain*. 2014;137(Pt 1):183–196.
45. Spencer SS, Kim J, Spencer DD. Ictal spikes: A marker of specific hippocampal cell loss. *Electroencephalogr Clin Neurophysiol*. 1992; 83(2):104–111.
46. Saggio ML, Crisp D, Scott JM, et al. A taxonomy of seizure dynamotypes. *eLife*. 2020;9.
47. Jirsa VK, Stacey WC, Quilichini PP, Ivanov AI, Bernard C. On the nature of seizure dynamics. *Brain*. 2014;137(Pt 8):2210–2230.
48. Karoly PJ, Kuhlmann L, Soudry D, et al. Seizure pathways: A model-based investigation. *PLoS Comput Biol*. 2018;14(10): e1006403.
49. Wang Y, Trevelyan AJ, Valentin A, et al. Mechanisms underlying different onset patterns of focal seizures. *PLoS Comput Biol*. 2017;13(5):e1005475.
50. Faught E, Kuzniecky RI, Hurst DC. Ictal EEG wave forms from epidural electrodes predictive of seizure control after temporal lobectomy. *Electroencephalogr Clin Neurophysiol*. 1992;83(4): 229–235.
51. Huberfeld G, Menendez de la Prida L, Pallud J, et al. Glutamatergic pre-ictal discharges emerge at the transition to seizure in human epilepsy. *Nat Neurosci*. 2011;14(5):627–634.
52. Lee SA, Spencer DD, Spencer SS. Intracranial EEG seizure-onset patterns in neocortical epilepsy. *Epilepsia*. 2000;41(3):297–307.
53. Lillis KP, Wang Z, Mail M, et al. Evolution of network synchronization during early epileptogenesis parallels synaptic circuit alterations. *J Neurosci*. 2015;35(27):9920–9934.
54. Memarian N, Madsen SK, Macey PM, et al. Ictal depth EEG and MRI structural evidence for two different epileptogenic networks in mesial temporal lobe epilepsy. *PLoS ONE*. 2015;10(4): e0123588.
55. Ogren JA, Bragin A, Wilson CL, et al. Three-dimensional hippocampal atrophy maps distinguish two common temporal lobe seizure-onset patterns. *Epilepsia*. 2009;50(6):1361–1370.
56. Schevon CA, Ng SK, Cappell J, et al. Microphysiology of epileptiform activity in human neocortex. *J Clin Neurophysiol*. 2008;25(6): 321–330.
57. Stead M, Bower M, Brinkmann BH, et al. Microseizures and the spatiotemporal scales of human partial epilepsy. *Brain*. 2010; 133(9):2789–2797.
58. Zhao C, Teng EM, Summers RG Jr, Ming GL, Gage FH. Distinct morphological stages of dentate granule neuron maturation in the adult mouse hippocampus. *J Neurosci*. 2006;26(1):3–11.
59. Espósito MS, Piatti VC, Laplagne DA, et al. Neuronal differentiation in the adult hippocampus recapitulates embryonic development. *J Neurosci*. 2005;25(44):10074–10086.
60. Jouny CC, Franaszczuk PJ, Bergey GK. Signal complexity and synchrony of epileptic seizures: Is there an identifiable preictal period? *Clin Neurophysiol*. 2005;116(3):552–558.
61. McIntosh AM, Averill CA, Kalnins RM, et al. Long-term seizure outcome and risk factors for recurrence after extratemporal epilepsy surgery. *Epilepsia*. 2012;53(6):970–978.